NASA TN D-1659

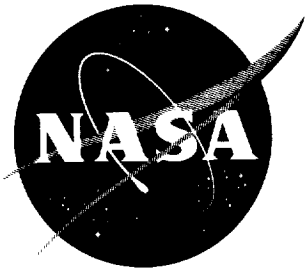

TECHNICAL NOTE
D-1659

EXPERIMENTAL EVALUATION OF A DIRECT-CURRENT LOW-PRESSURE PLASMA SOURCE

By Stanley Domitz

Lewis Research Center
Cleveland, Ohio

NATIONAL AERONAUTICS AND SPACE ADMINISTRATION
WASHINGTON

April 1963

Code 1

NATIONAL AERONAUTICS AND SPACE ADMINISTRATION

TECHNICAL NOTE D-1659

EXPERIMENTAL EVALUATION OF A DIRECT-CURRENT LOW-PRESSURE PLASMA SOURCE

By Stanley Domitz

SUMMARY

A plasma source, which consists of a hot-filament coaxial discharge in an axial magnetic field, was operated with argon gas. The quantities measured in the plasma beam were the magnitude plus spatial distribution of electron temperature, number density, and plasma potential. The plasma production efficiency is given as a function of the discharge parameters.

The plasma beam was found to be up to 10 percent ionized with a minimum energy cost of 125 electron volts per ion, excluding filament and magnet power.

INTRODUCTION

The plasma source described in this report was developed for use with a radio-frequency traveling-wave accelerator (ref. 1). For this application it was required that the source run continuously for long periods of time, have the capability of operating at low pressure (less than 1 micron Hg), and be easily adaptable to changes in the accelerator.

The general requirements for a plasma source are that it operate efficiently and provide the ionization required by the accelerator. To determine the local plasma properties and the energy required to produce an ion-electron pair, measurements were made using several diagnostic techniques. The techniques are standard except for a new type collector (total plasma probe), which is described in detail.

The plasma source consists of a hot-filament coaxial discharge in an axial magnetic field. The design of the source is based on that of reference 2, where a similar discharge is utilized as an ion source for an electrostatic accelerator. Other pertinent studies of a discharge in a magnetic field are references 3 to 5.

One of the major power losses of a plasma accelerator is due to the ionization process. It is believed that the study of a plasma source as a component will be helpful in the design of plasma propulsion systems.

SYMBOLS

A	area
B	magnetic field
e	electronic charge
F	flux ratio
J	current
J_m	total probe current
J_o	Langmuir probe saturation current
j	current density
K	number of ions per primary electron
m	electron mass
$\dot{N}_+$	total ion production rate
n	electron density
P	ion fraction
R	radius
R_c	electron cyclotron radius
T_e	electron temperature
t	time
U	electron energy
$\bar{U}$	mean random electron energy
V	voltage
ΔV_d	average axial acceleration potential
ΔV_r	radial plasma potential difference
v	velocity
$\bar{v}$	average velocity
ϵ	effective ionization potential

η utilization factor for primary electrons

$\varphi(U)$ energy distribution function

Subscripts:

a anode

b backplate

e emitted electron

p plasma

γ radial

0 neutral

+ ion

- electron

THEORY OF OPERATION

The plasma source investigated is shown in figure 1. Electrons are emitted from a hot filament along the axis of the cylindrical anode. The pressure is adjusted so that the mean free path is greater than the dimensions of the apparatus. An axial magnetic field causes the electrons to spiral around the field lines until they reach the anode by means of collisions. Electrons are free to move along the axis but oscillate between the reflecting plate at one end of the source and the reflecting potential gradient that exists in the plasma outside the source.

Primary electrons emitted thermionically from the filament are accelerated through the space-charge sheath surrounding the filament (sketch (a), region A). The energy that they receive is given by the potential difference between the cathode and the plasma, which is approximately equal to the total applied potential difference. A small potential difference across the plasma, region B, is sufficient to conduct the electron current. At the anode, region C, a sheath forms to reflect a fraction of the electrons, since the arrival rate of electrons due to random electron motion is greater than the current.

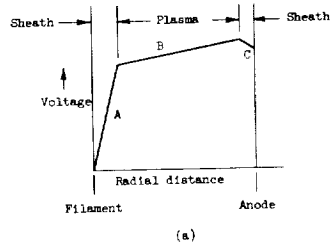

(a)

From sketch (a) it can be seen that most of the power put into the discharge appears at the voltage drop near the filament. This power is predominantly converted into the kinetic energy of the primary electrons. The problem of designing an efficient source is one of controlling the motions of the primary electrons so as to maximize the ion production rate. In competition with the ion production process, power is lost in excitation collisions, in the acceleration of ions through the potential gradients, and in the conduction of heat to the walls by energetic electrons.

Ion Production

An analysis of the ion production is complicated by the fact that the various collision cross sections are dependent on the electron energy, which is not known throughout the discharge.

If it is assumed that ionization is produced by collision with primary electrons, the ion production rate is given by

$$\dot{N}_+ = \eta J_e K \tag{1}$$

where J_e is the emitted current of primary electrons of a given energy, η is the fraction of the electron beam utilized in collision processes with neutrals, and K is the number of ions produced per primary electron.

In order to compare equation (1) with experiment, it is convenient to introduce the effective ionization potential ϵ, defined as

$$\epsilon = \frac{U}{K} \tag{2}$$

where U is the initial electron energy. The effective ionization potential is the minimum energy required to produce an ion-electron pair and is always larger than the ionization potential because excitation and elastic losses are present. Sketch (b) shows the experimental values of ϵ taken from reference 6.

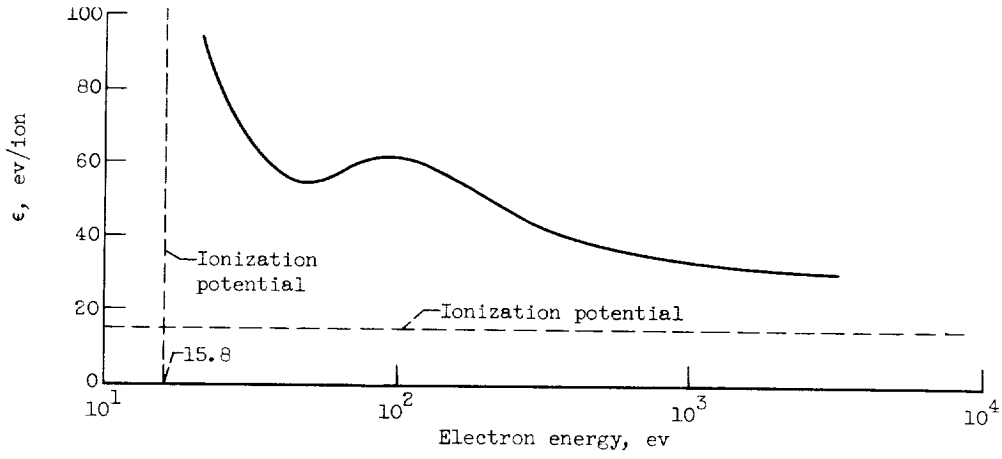

(b)

Combining equations (1) and (2) gives

$$\dot{N}_+ = \eta J_e \frac{U}{\epsilon} \tag{3}$$

The terms in equation (3) can be evaluated, in some cases only approximately, but the evaluation is a check on several independent experimental measurements.

In a steady-state discharge with no volume recombination, the total ion production rate is equal to the diffusion rate of ions to the boundaries of the apparatus. For the configuration shown in figure (1), the flux of ions leaving the discharge can be measured in two places: outside the source and at the rear plate when the plate is biased negatively to repel electrons. This represents the total ion current if the flow of ions to the anode and filament is negligible.

Ions can only reach the anode if they are produced at the anode sheath. Elsewhere in the discharge the plasma potential gradients tend to move ions away from the anode. The ion current to the filament was also considered to be small. This assumption was substantiated by measurements made in the discharge with a negatively biased probe that collected saturation ion current.

Utilization of High-Energy Electrons

As discussed previously, most of the power put into the discharge appears in the kinetic energy of the primary electrons. The electrons either escape or suffer energy losses in inelastic collisions until their energy falls below the lowest excitation potential, after which they play a passive role until removed by the radial electric field.

Radial losses. - In a cylindrical geometry, primary electrons move across the magnetic field and reach the wall by means of collisions. An electron must make at least one collision to sustain the discharge, and several collisions are required to utilize the electron energy. The electron cyclotron radius R_c should therefore be less than one-half the anode radius R_a as shown in sketch (c).

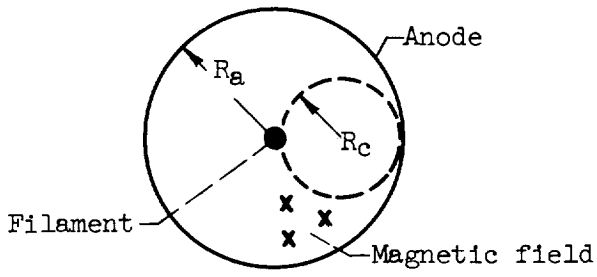

(c)

The function of the magnetic field is to control R_c ($R_c \propto 1/B$). The magnetic field cannot be made arbitrarily large to ensure complete utilization of the electron energy; an optimum exists. As the field is increased, the radial potential drop increases (increased resistivity), which results in a lower primary electron energy and a loss of power in resistive heating.

Axial losses. - In the usual form of an oscillating electron, discharge electrons are reflected from the chamber end plates. When one of the end plates is removed, an interesting phenomenon occurs. An axial potential gradient is established that reflects electrons and accelerates ions. A similar effect has been investigated (ref. 5) in a Penning discharge that is used as a plasma accelerator.

In the source described here the gradient is not imposed on the plasma by means of electrodes. The gradient is the solution the plasma adopts to adjust to the boundary condition that no net current can leave the device, and a certain fraction of electrons must therefore be reflected. The power required to accelerate ions must come from the input power, which is originally imparted to the beam of primary electrons. A fraction of the electron energy, therefore, becomes unavailable for ionization; however, there is also an advantage associated with the existence of an axial potential gradient. When ions are created in the region of the gradient, they are prevented from drifting back into the source; therefore, the downstream flow of ions is larger than the upstream loss.

EXPERIMENTAL APPARATUS AND PROCEDURE

Plasma Source

The source (fig. 1) consists of a 2.75-inch-diameter stainless steel cylinder 3 inches long with a 0.010-inch-diameter tungsten wire mounted along the axis and a rear plate that is a combined reflecting cathode and gas diffuser. The entire assembly is mounted on a flange that provides mechanical support and the connections for the electrical and gas supply. The assembly fits inside one end of a 3-inch-diameter pyrex pipe 1 foot long with the flange sealing the end of the pipe. Three 5-inch-diameter magnetic-field coils are mounted on the outside of the glass pipe. The magnetic-field range is 0 to 200 gauss at the center of the source; the axial field distribution is shown in figure 2.

Vacuum Facility

The glass pipe mentioned previously is connected to a 6-inch pyrex cross that provides the entrance ports for the vacuum gages, the roughing-down line, and the diagnostic probes. A 6-inch gate valve with on-off operation separates the 6-inch cross from the vacuum facility. A 5-foot-diameter stainless steel tank 15 feet long is pumped by four 32-inch diffusion pumps, with a combined pumping speed of 100,000 liters per second. This tank is one of several facilities in use at the Lewis Research Center for electric rocket research. Reference 7 describes the vacuum system in more detail.

Argon gas used for the experiment was supplied from a commercial cylinder, was filtered and dried, and then was admitted through a variable leak.

Power supplies were standard d-c supplies with extra filtering added to bring the ripple down to less than 0.1 percent. Figure 2 shows the electric schematic of the apparatus.

To operate the plasma source, the glass hardware outside the large vacuum tank is roughed down to a few microns of pressure and then opened to the tank. The tank itself is usually kept at a pressure of the order of 10^{-7} millimeter of mercury. This arrangement is convenient for small-scale experiments that require frequent shutdowns (for probe changes, etc.), since there is no waiting time to begin a run.

Gas flow is established with a variable leak. Actually, the pressure in the apparatus is adjusted with the gas flow. The physical phenomena of the plasma are pressure dependent, and pressure is therefore a more desirable variable.

DIAGNOSTIC METHODS AND EQUIPMENT

Langmuir Probe

The Langmuir probe is a standard instrument for determining the electron temperature, electron density, and plasma potential (refs. 8 and 9). It is simply a bare wire inserted in the plasma; the current collected by the probe is a function of the probe potential. Thus, all the information obtained is deduced from the voltage-current curve.

At plasma potential (V_p) the probe collects the random electron current

$$J_o = ne \frac{\overline{v}}{4} A \tag{4}$$

where $\overline{v}$ is the average electron velocity.

If the probe is biased negatively to the plasma potential, electrons are reflected, and the collected current decreases with the applied voltage. If a Maxwellian distribution of electrons is assumed,

$$J = J_o \exp \frac{V - V_p}{T_e} \tag{5}$$

where T_e is the electron temperature in volts. Taking the logarithm of both sides of equation (5) results in

$$\log J = \log J_o + \frac{V - V_p}{T_e} \log e \tag{6}$$

Thus, the electron temperature can be calculated from the slope of the

linear portion of a semilog plot of the collected current against probe voltage. The point where the curve deviates from a straight line is taken to be plasma potential. Number density is then obtained from equation (4) by taking the average velocity to be $\bar{v} = \sqrt{\frac{8eT_e}{\pi m}}$.

In reference 10 it is pointed out that the apparent linear relation between probe voltage and the logarithm of the probe current is not a sensitive test for a Maxwellian distribution. Another method for determining the electron energy distribution from an analysis of the probe trace is the Druyvesteyn method, which uses the following equation:

$$n\varphi(U) = \frac{2}{Ae}\left(\frac{2mU}{e}\right)^{1/2} \frac{d^2j}{dV^2} \tag{7}$$

where $U = V_p - V$, $n\varphi(U)$ is the electron density within an energy increment dU, and d^2J/dV^2 is the second derivative of the Langmuir probe trace. The derivation assumes that the electron velocities are isotropic (for other than spherical probes) and that the plasma potential can be determined.

By definition, number density is

$$n = \int_0^\infty n\varphi(U)\, dU \tag{8}$$

and the mean random electron energy $\bar{U}$ is

$$\bar{U} = \frac{\int_0^\infty n\varphi(U)U\, dU}{\int_0^\infty n\varphi(U)dU} \tag{9}$$

which can be found graphically. The problem of obtaining the second derivative of the probe curve has discouraged wider use of the Druyvesteyn method. Further discussion of the subject can be found in reference 10.

The Langmuir probe and circuit diagram are shown in figure 3. Probe voltage was varied continuously by means of a motor-driven potentiometer, and the voltage-current trace was recorded on an X-Y plotter. As auxiliary equipment, a logarithmic converter was found to be useful; the logarithm of current as a function of voltage was plotted directly.

Hot Probe

For determining plasma potential gradients where a large number of data

points are taken, the hot probe, or electron-emitting probe, is more convenient to use than a Langmuir probe. In addition, the hot probe defines plasma potential in a consistent way from point to point, whereas the Langmuir probe requires the analysis of a curve for each data point, and the location of plasma potential becomes a matter of judgment.

The hot probe works on the principle that electrons will be emitted from the heated filament only when the probe bias is negative to plasma potential. The emitter current falls to zero at plasma potential.

The relation between the hot and cold (Langmuir) probe is shown in figure 4. The figure also shows that the hot-probe floating potential is close to plasma potential. Thus, for a rough determination of plasma potential, a floating hot probe is adequate in many situations.

Figure 5 shows the circuit diagram and probe details. The probe is heated by an a-c current. A measurement is made by varying the probe bias until no change in probe current is recorded when the probe heating current is switched on and off. This point is taken to be plasma potential. Further discussion of errors and other details can be found in references 11 and 12.

One common problem with hot probes is that they burn up easily because of the high-temperature operation. The probe construction shown in figure 5 gave the best results. To prevent the lead-in wire, which is copper, from melting, a transition wire of molybdenum was used between the tungsten and copper.

Total Plasma Probe

In order to obtain quantitative data concerning the output of plasma from the source, a collector was developed to measure plasma production without blocking the flow of gas. The collector is essentially a floating double probe (ref. 13) with unequal areas.

As shown in figure 6, the large area is a cylinder 9 inches long lining the inside of the glass pipe. A 1/8-inch-diameter rod runs along the axis of the cylinder. Since the probe is floating, it draws no net current from the discharge. When the potential difference is varied between the rod and cylinder, a double probe curve is generated as shown in sketch (d).

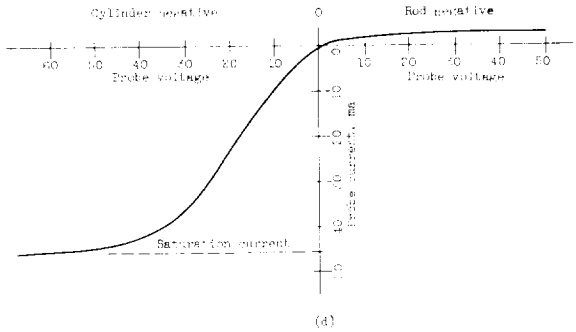

(d)

The probe is operated with a cylinder negative to repel electrons and collect the saturation ion current. When this is done, the center rod rises in potential to collect the necessary electron current to balance the sum of the ion currents to both the cylinder and the rod. The entire probe is floating and can collect no net current. Sketch (e) shows schematically the currents measured.

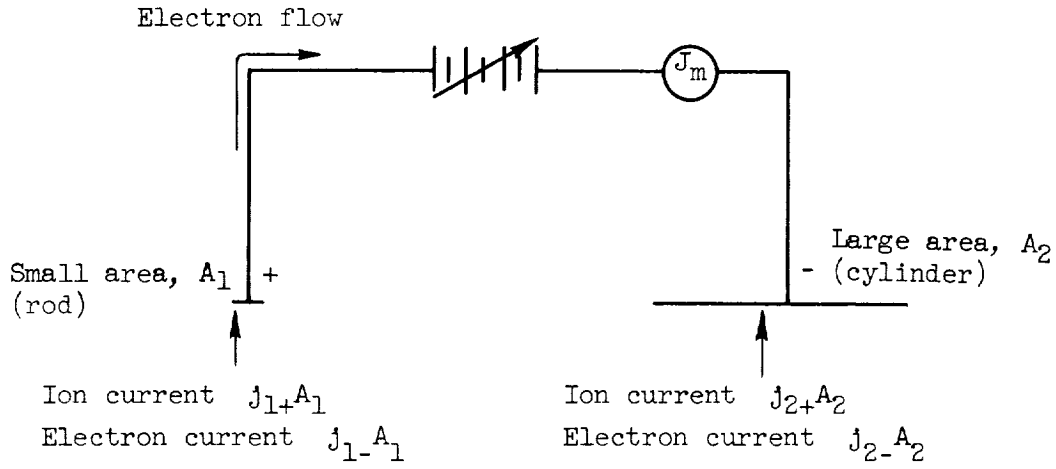

(e)

The measured current is

$$J_m = j_{2+}A_2 - j_{2-}A_2 = j_{1-}A_1 - j_{1+}A_1$$

When the large cylinder reaches ion saturation, $j_{2-}A_2 \approx 0$. The total ion current leaving the source is

$$J_+ = j_{2+}A_2 + j_{1+}A_1 + J_l$$

where J_l is the current of ions lost through the open end. Therefore,

$$J_m = J_+ - j_{1+}A_1 - J_l$$

If $A_2 \gg A_1$, $j_{1+} \approx j_{2+}$, and $J_l/J_m \ll 1$, the measured current is approximately the total ion current.

The amount of plasma escaping through the end of the cylinder (J_l) depends on the pressure but in the normal operating range was not large, since a 50-percent increase in cylinder length increased the measured current by only a few percent.

An operational limit of the probe would occur if the center rod reached electron saturation before the cylinder became ion saturated. This point might be reached at a very large area ratio, but was not observed in the experiments reported here.

Another possible error is the effect of secondary electrons emitted from the cylinder because of ionic bombardment. At normal operating voltage, up to 60 volts, the effect is small.

Although the probe does have some effect on the discharge, since it influences the motion of the high-energy electrons, the results obtained with the probe seem to be reasonable. More work is required to establish its absolute accuracy.

Noise Measurements

Noise, or voltage fluctuations, in the plasma source is of interest when the noise becomes competitive with d-c fields. In this case, calculations using measured d-c potentials would be misleading; the a-c processes may be of equal importance.

To measure noise, a bare-wire probe biased to plasma potential was used, and the output was read from an oscilloscope. The bias voltage is necessary to prevent signal attenuation through the plasma sheath surrounding the probe. At plasma potential the sheath disappears, and the measured voltage fluctuations reach peak intensity.

This method also suggests the possibility of finding plasma potential from the peak noise intensity. Reference 14 describes the result of applying such a technique.

Microwave Interferometer

A rough check of the electron number density data was made using a K-band microwave interferometer across a diameter of the source. The data themselves are not reported here, since they provided no new information on the density distribution with radius and because at low operating pressures the phase shifts were small and not too reliable. Details of the equipment and methods used can be found in reference 15.

DISCUSSION OF RESULTS

Two types of data are presented: (1) local plasma properties, such as number density, electron temperature, plasma potential, and noise; and (2) the current of charged particles collected by the total plasma probe in the region downstream of the plasma source. In both cases, the experimental parameters were anode voltage, anode current, magnetic field, and argon gas pressure.

Typical variation of electron density measured with a Langmuir probe is shown in figure 7. The data were taken in the center of the glass pipe 1 inch from the source. The discharge parameters were held constant (except where they are displayed as the variable) at the following values: anode potential, 50 volts; anode current, 1 ampere; magnetic field, 50 gauss; and gas pressure, 1.5×10^{-4} millimeter of mercury.

As shown in figure 7(b) electron density is primarily controlled by the emission current. The variation of electron density with anode potential (fig. 7(a)) is fairly flat in the region of operation. In figure 7(c) electron density drops to very low levels (in some cases the discharge is extinguished) at low magnetic field strength. The drop in density coincides with the fact that at about 8 gauss the electron cyclotron radius is approximately equal to one-half the anode radius, which would be a possible cutoff point for plasma production. In figure 7(d) electron density rapidly increases with pressure up to a point where the primary electron beam becomes nearly fully utilized for ion production. As a result of the nonlinear increase with pressure, there is a point of maximum percent ionization, shown by the solid symbol.

Figure 8 shows the radial variation of number density and electron temperature 1 inch from the source. The magnetic field changes the shape of the density distribution (fig. 8(a)). In fact, at very strong magnetic fields the discharge is confined to a pencillike beam in the center of the pipe. For this reason, the values of number density measured at a single point are not always a reliable indication of how the overall ion production varies with the discharge parameters. The integrated output measured with the total plasma probe is of more significance. The radial profile of electron temperature (fig. 8(b)) shows that electron energy is degraded as the electrons diffuse to the wall.

Electron temperature was found to be primarily a function of pressure, as shown in figure 9. However, at the lower pressures Langmuir probe curves indicated a departure from a Maxwellian distribution. In order to investigate the electron energy distribution the Druyvesteyn method was used (eq. (7)). The result is shown in figure 10 where the curves are normalized for comparison with a Maxwellian distribution. The second derivative of the voltage current curve was taken graphically, and the number density and average electron energy were also found graphically by using equations (8) and (9).

Figure 10 indicates that a large population of low-energy electrons exists in the discharge when compared with a Maxwellian distribution. This coincides with the fact that low-energy electrons are trapped in the discharge because of the existence of reflecting sheaths at every boundary; however, some caution should be used in interpreting these results. If a distribution of high-energy electrons were present along with a Maxwellian distribution, the procedure used to normalize the curves would tend to distort the Maxwellian portion.

It is interesting to note that the values for number density and average electron energy found with the Druyvesteyn method agreed within 10 percent with the values found with the Langmuir method even when the latter was questionable because of the existence of a non-Maxwellian electron energy distribution.

The abovementioned effects were not investigated in greater detail because of the tedious nature of the graphical computations. To exploit the Druyvesteyn method fully, automatic equipment should be used to reduce the data.

Axial and radial plasma potentials that were measured with a hot probe are shown in figures 11 and 12. In figure 11 the axial potential gradient is seen to increase at low pressure but varies only slightly with magnetic field strength. Ions are accelerated by the gradient, which suggests a possible appli-

cation for the device as a plasma accelerator. The magnitude of the total acceleration potential difference could not usually be determined because of the physical limits of the apparatus. However, it is reasonable to assume that the acceleration voltage is on the order of the primary electron energy, as shown in the lower curve of figure 11. No attempt was made to optimize the device as an accelerator.

The radial potential drop shown in figure 12 is small, on the order of 1 volt except at larger magnetic fields. As shown in the figure, with the stronger fields the gradient increases at the expense of the initial electron energy, which is determined by the plasma potential at the filament.

Voltage oscillations, or noise measurements, were taken 1 inch from the source over a frequency range up to 30 megacycles (fig. 13). Inside the source the signal strength (peak to peak) was about twice as great and increased from the center to the wall. The noise amplitude increased with the magnetic field and varied inversely with gas pressure. The noise amplitude is of the same order as the voltage drop across the plasma and may be of equal importance in determining electron motions.

Another local property of the plasma that is of interest is the percent ionization, the fraction of gas molecules that are ionized. The neutral density is taken to be the density in the source before the discharge is initiated. The maximum value was about 5 to 10 percent. This number is not precise because the probes become damaged when operating in the region of maximum ionization, and only a few data points were taken.

Percent ionization may not be as important as another number, the ratio of ion flux to total flux F:

$$F = \frac{n_+ v_+}{n_+ v_+ + n_0 v_0} \tag{11}$$

where $n_0 v_0$ is the neutral flux.

Equation (11) can be rewritten

$$F = \frac{P}{\frac{v_0}{v_+} + P\left(1 - \frac{v_0}{v_+}\right)} \tag{12}$$

where P = ion fraction = $n_+/(n_+ + n_0)$. When $v_0 = v_+$, F = P; however, for any P, F approaches unity as v_0/v_+ approaches zero.

In figure 14 the flux ratio F is plotted against the velocity ratio v_+/v_0 with the ion fraction P as a parameter. It can be seen that, when the ion velocity is much greater than the neutral velocity, the flux ratio is large even at low percentage ionization. Thus, for the case where a gradient exists to accelerate ions, it may not be necessary to provide a highly ionized plasma in the source.

Plasma Production

Data for figures 15 and 16 were taken with the total plasma probe. Figure 15 shows the form in which data are plotted to arrive at the energy required to produce a collected ion-electron pair. At a constant pressure, 3×10^{-4} millimeter of mercury, the discharge parameters, anode voltage, anode current, and magnetic field, are varied, while the probe current is kept constant. At any point on the curve the product of anode voltage and current is the input power to the gas, and the energy per particle is $ev/ion = J_aV_a/J_m$ where J_m is the probe current.

The input power J_aV_a does not include the power used for filament heating and the magnetic field. The reasons for this omission are: (1) No attempt was made to optimize the design of the magnetic field coils and filament, and (2) it was desirable to relate the data directly to the energy of the primary electrons. The effect of the discharge parameters on the ion production energy is shown in figure 16, where one parameter was varied at a time while the others were held constant at the values shown.

In figure 16(a) the energy cost per ion begins to rise sharply below an anode potential of 40 volts; below 30 volts, the discharge operates erratically. The variation with anode current (fig. 16(b)) is fairly flat at the pressure shown, 3×10^{-4} millimeter of mercury; however, at lower pressure an optimum occurs above which electrons cannot be utilized as effectively.

The energy cost with magnetic field variation (fig. 16(c)) becomes very high as the electron cyclotron radius approaches one-half the anode radius at about 8 gauss. The shape of the curve (fig. 16(c)) should be explainable in terms of the number of collisions needed to utilize the electron energy. However, because the magnetic field is divergent, the electron cyclotron radius varies along the axis, which precludes a simple calculation. The value for the field in figure 16(c) is for the center of the source.

A low pressure limit on the operation of the source (fig. 16(d)) is reached below 0.1 micron of mercury. Although the energy cost decreases with increasing pressure, the point of maximum percent ionization for these conditions, shown by the solid symbol, occurs at 260 electron volts per ion.

The data shown in figure 16 are typical, but the interaction between the parameters is complicated. In general, however, an optimum exists where the energy per collected ion is on the order of 150 electron volts, with the lowest measured value being about 125 electron volts.

The region of efficient source operation was found to be in the following range: anode voltage, 40 to 70 volts; anode current, up to 5 amperes; magnetic field, 35 to 100 gauss; and pressure, above 0.1 micron of mercury.

Energy Balance

As mentioned previously, the sum of the currents to the total plasma probe and the rear plate was taken to be the total ion production rate. An energy bal-

ance was made for a sample case shown in the following table, and the energy not otherwise accounted for was assumed to be required for the ionization process. In effect, equation (3), which can be written as $\dot{N}_+ = \eta J_A V_A/\epsilon$ was solved experimentally to obtain a value for ϵ, the effective ionization potential. This serves as a check on the many assumptions that were made.

Quantity	Symbol	Current, amp	Potential, volts	Power, watts
Anode current	J_a	1		
Anode voltage	V_a		50	
Input power	$J_a V_a$			50
Radial plasma potential difference	ΔV_r		1	
Resistive power	$J_a\ \Delta V_r$			1
Electron temperature	T_e		8	
Thermal electron loss	$J_a T_e$			8
Downstream ion current (total plasma probe)	J_m	0.32		
Average downstream acceleration potential	ΔV_d		[a]28	
Downstream acceleration power	$J_m\ \Delta V_d$			8.9
Backplate ion current	J_b	0.13		
Backplate potential drop	ΔV_b		40	
Upstream acceleration power	$J_b\ \Delta V_b$			5.2
Power left for ionization, $J_a V_a - J_a(\Delta V_r + T_e) - J_m\ \Delta V_d - J_b\ \Delta V_b$	$\eta J_a V_a$			26.9
Effective ionization potential, $\eta J_a V_a/(J_m + J_b) \approx \eta J_e U/\dot{N}_+$	ϵ		60	

[a]Adjusted potential, to take into account the axial distribution of ion production.

The value for ϵ given in reference 16 is 55 electron volts for 50-volt primary electrons. Although the energy balance is only a first approximation, it is believed that the procedure is worthwhile to find out which processes deserve further theoretical and experimental study.

CONCLUDING REMARKS

An experimental study of a low-pressure d-c plasma source using argon gas has been conducted. Local plasma properties and total plasma output have been investigated in order to characterize the performance of a plasma source and to evaluate diagnostic techniques.

The device was found to be a convenient source of partially ionized (up to 10 percent) argon at pressures from 0.1 to 1 micron of mercury and power input on the order of 50 to 250 watts.

Electron temperature, which varied inversely with gas pressure, was in the range of 3 to 11 electron volts.

Axial potential gradients exist in the plasma beam. As a result, the ion flux can be larger than the neutral flux, even at a low ionization percentage.

The axial acceleration of ions also suggests application as a plasma accelerator. The radial potential difference across the plasma was on the order of a few volts and of the same magnitude as potential oscillations in the plasma.

From data taken with a total plasma probe the minimum energy cost of delivering an ion-electron pair is about 125 electron volts. The minimum energy cost was about $2\frac{1}{2}$ times the effective ionization potential.

Lewis Research Center
National Aeronautics and Space Administration
Cleveland, Ohio, December 10, 1962

REFERENCES

1. Jones, Robert E., and Palmer, Raymond W.: Traveling Wave Plasma Engine Program at NASA Lewis Research Center. Paper Presented at Third Annual Conf. on Eng. Magnetohydrodynamics, Univ. Rochester, Mar. 28-29, 1962.

2. Kaufman, Harold R.: An Ion Rocket with an Electron-Bombardment Ion Source. NASA TN D-585, 1961.

3. Gardner, A. L., et al.: P-4 - A Steady-State Plasma System. UCRL-5904, Radiation Lab., Univ. Calif., May 1960.

4. Guthrie, A., and Wakerling, R. K., eds.: The Characteristics of Electrical Discharges in Magnetic Fields. McGraw-Hill Book Co., Inc., 1949.

5. Meyerand, R. G., Jr., Salz, F., Lary, E. C., and Walch, A. P.: Electrostatic Potential Gradients in a Nonthermal Plasma. Proc. Fifth Int. Conf. on Ionization Phenomena in Gases, Munich, 1961.

6. Von Engel, A.: Ionized Gases. Clarendon Press (Oxford), 1955, p. 55.

7. Keller, Thomas A.: NASA Electric Rocket Test Facilities. Seventh Nat. Symposium on Vacuum Tech. Trans., Pergamon Press, 1960, pp. 161-167.

8. Langmuir, I., and Mott-Smith, H.: Studies of Electric Discharges in Gases at Low Pressures. General Electric Rev., vol. 27, no. 7, July 1924, pp. 449-455.

9. Verweij, W.: Probe Measurements and Determination of Electron Mobility in the Positive Column of Low-Pressure Mercury-Argon Discharges. Res. Reps. Supplements, no. 2, Phillips Res. Labs., 1961.

10. Boyd, R. L. F., and Twiddy, N. D.: Electron Energy Distributions in Plasmas. Proc. Roy. Soc. (London), ser. A, vol. 250, no. 1260, Feb. 1959, pp. 53-69.

11. Gabovich, M. D., Bartnovskii, D. A., and Fedorus, Z. P.: Droop in the Axial Potential of a Discharge with the Electron Oscillation in a Magnetic Field. Trans. from Zhur. Tekh. Fiz., vol. 30, no. 3, Mar. 1960, pp. 345-353.

12. Kistemaker, J., and Snieder, J.: Some Measurements on a Not Selfsustaining Gas Discharge, with an Axial Magnetic Field. Physica, vol. 19, 1953, pp. 950-960.

13. Johnson, E. O., and Malter, L.: A Floating Double Probe Method for Measurements in Gas Discharges. Phys. Rev., vol. 80, no. 1, Oct. 1, 1950, pp. 58-68.

14. Zaitsev, A. A., Ya Vasil'eva, M., and Mnev, V. N.: Possibility of Determining the Potential Distribution of a Plasma from the Characteristics of the Noise Generated in a Gaseous Discharge. Soviet Phys., JETP, vol. 9, no. 5, Nov. 1959, p. 1130.

15. Kuhns, Perry: Microwave Interferometer Measurements of Electron-Ion Recombination in Nitrogen, Air, and Argon. NASA TN D-1191, 1962.

16. Brown, Sanborn Conner: Basic Data of Plasma Physics. Tech. Press, M.I.T., 1959.

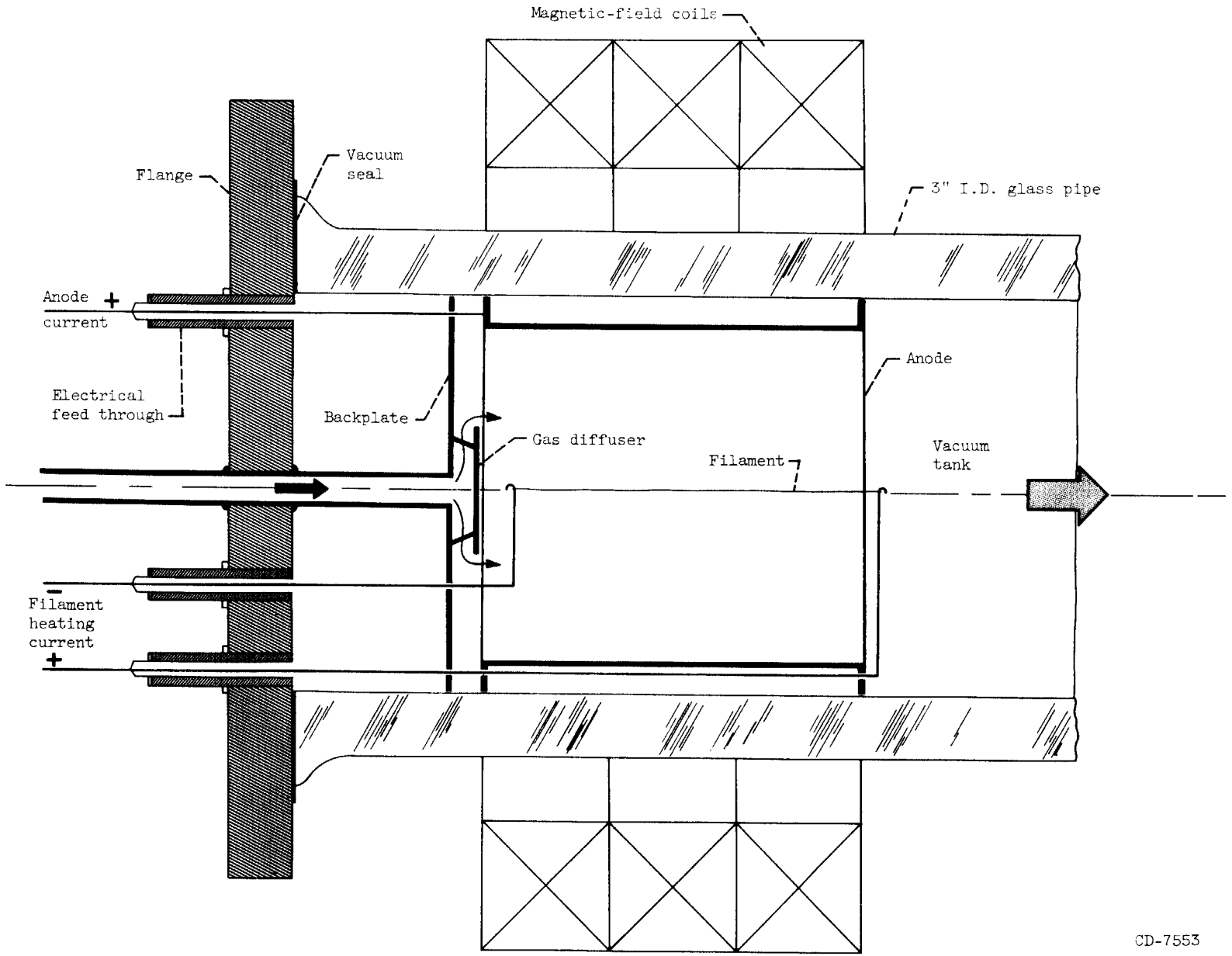

Figure 1. - Plasma source.

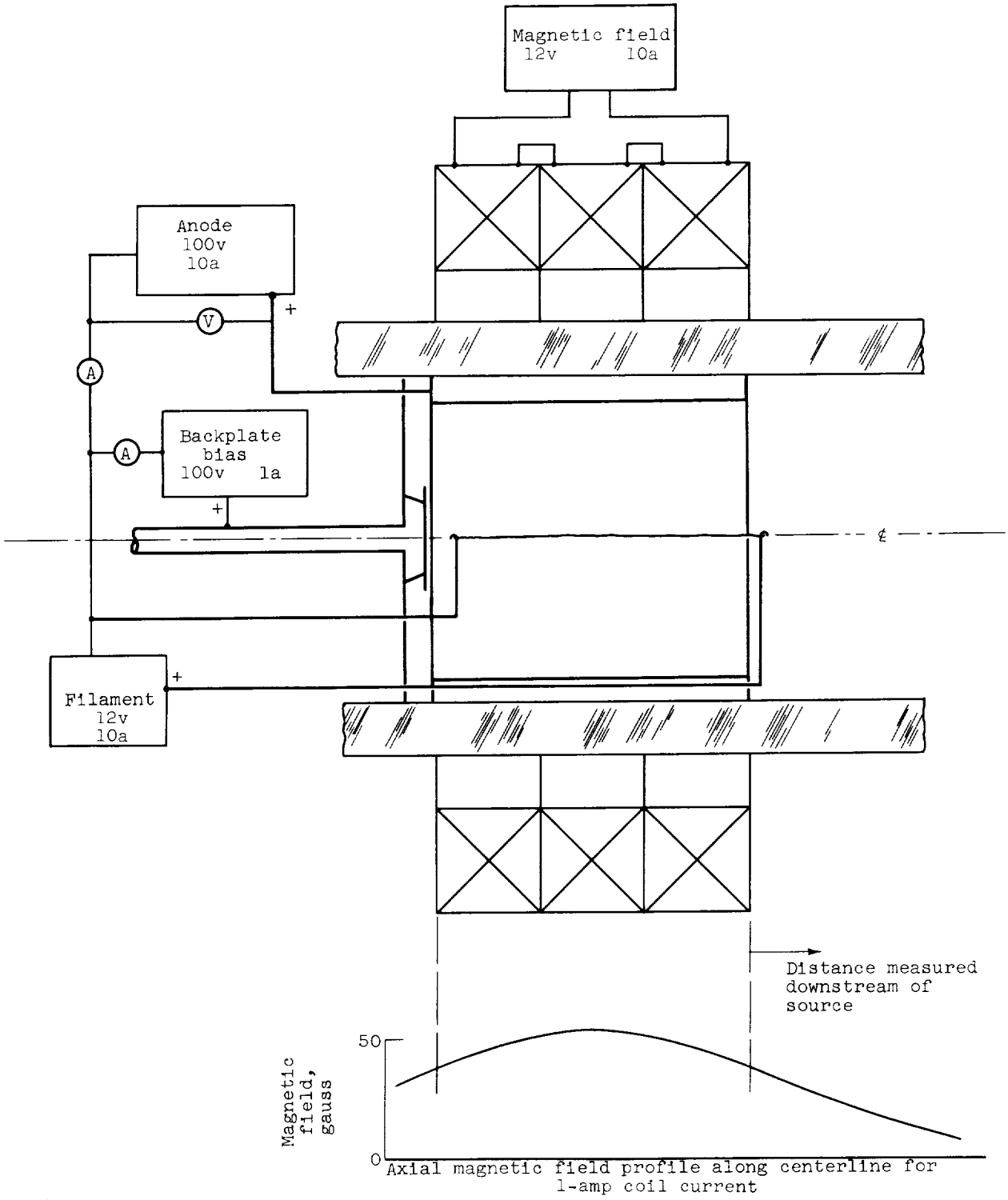

Figure 2. - Plasma source, electrical circuit, and magnetic field distribution.

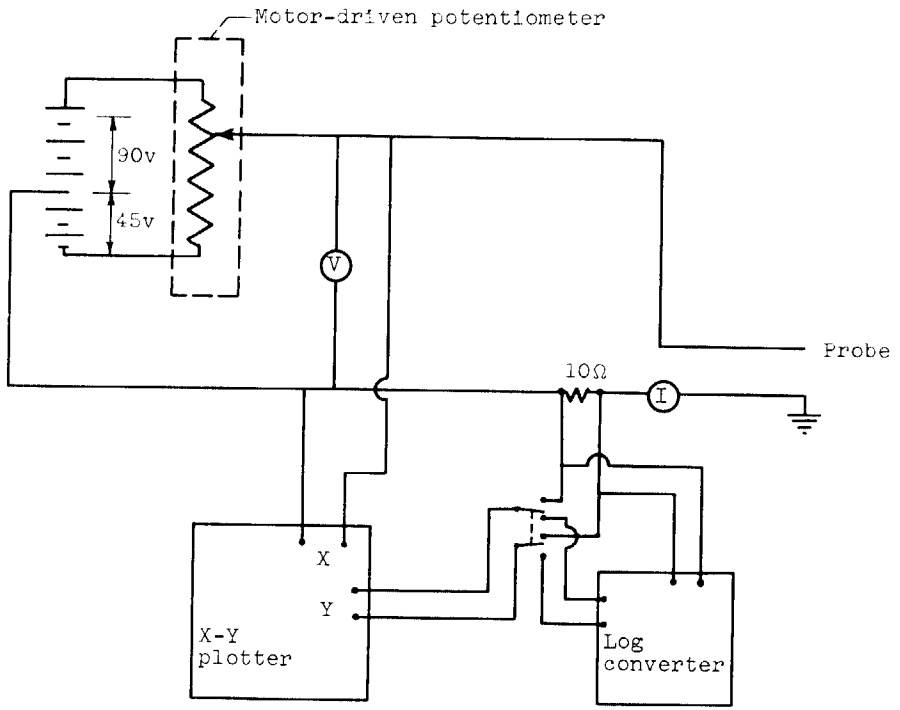

(a) Circuit.

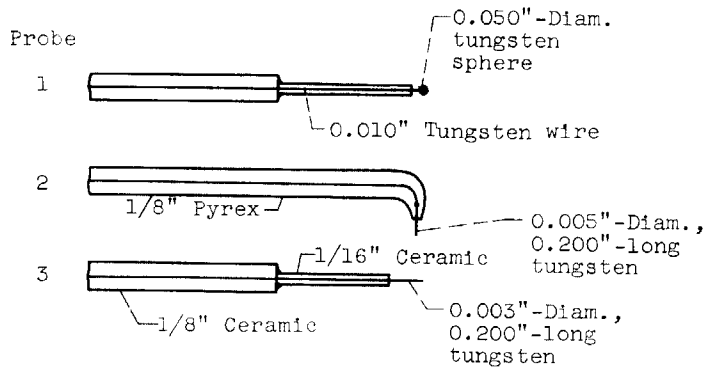

(b) Probes.

Figure 3. - Langmuir probe and circuit diagram.

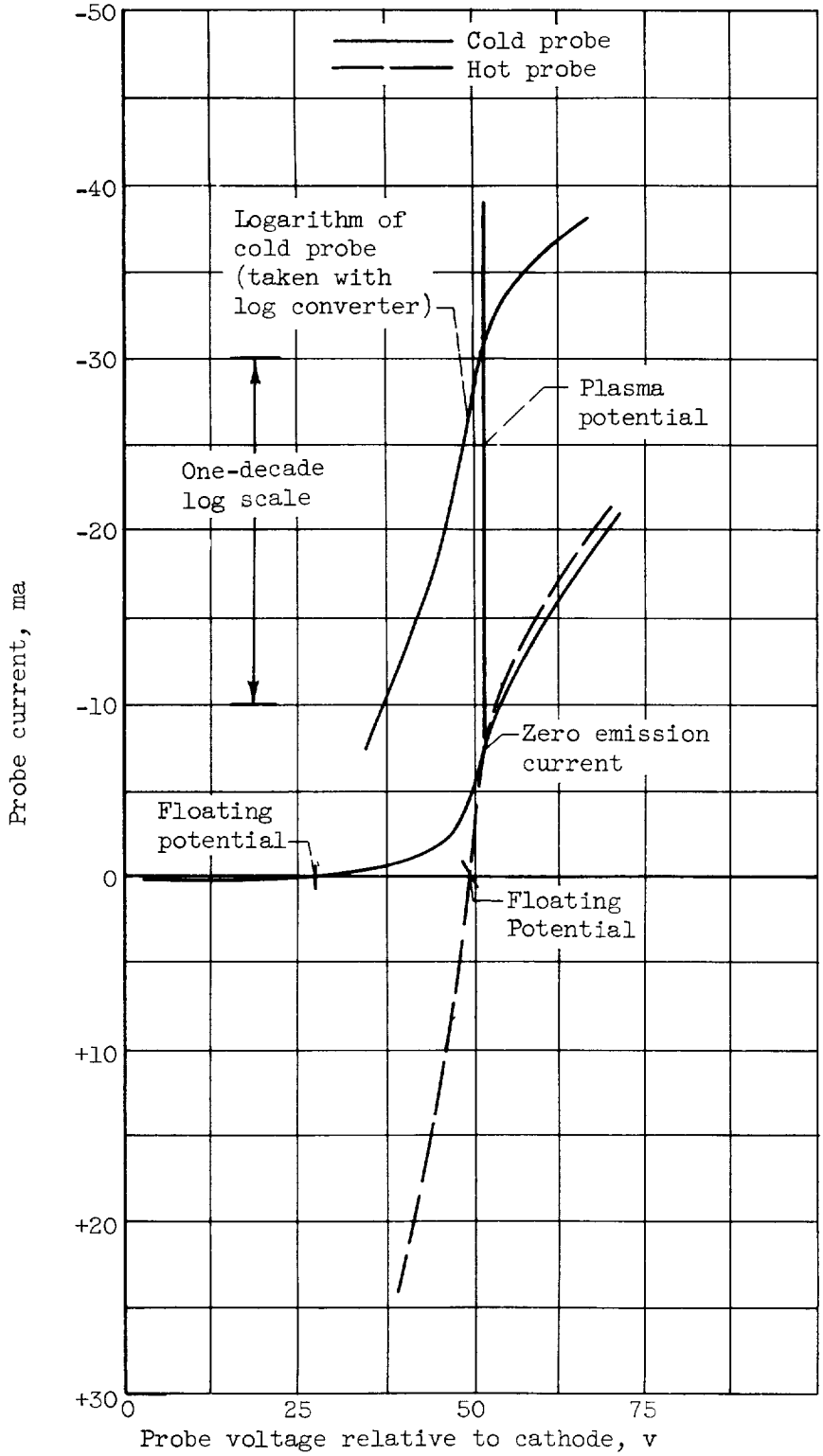

Figure 4. - Typical data taken with X-Y plotter showing relation of hot- and cold-probe curves.

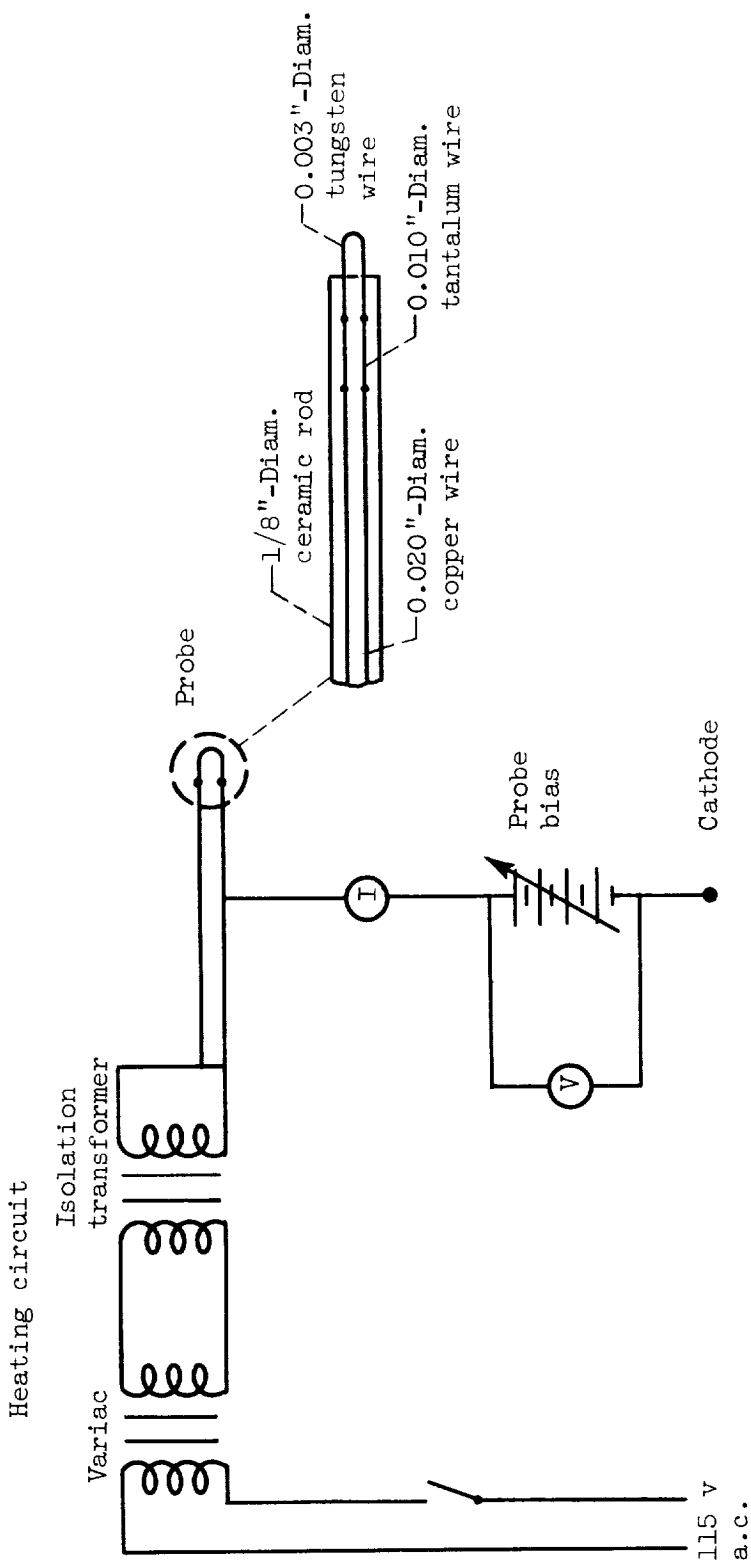

Figure 5. - Hot-probe circuit.

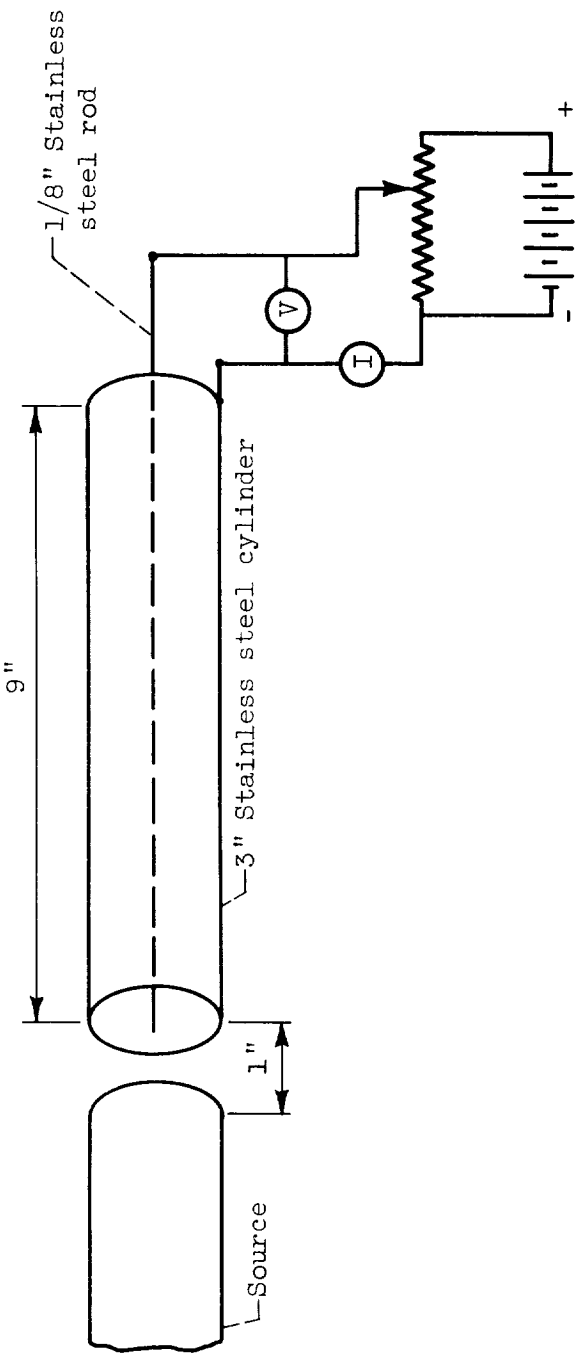

Figure 6. - Total plasma probe.

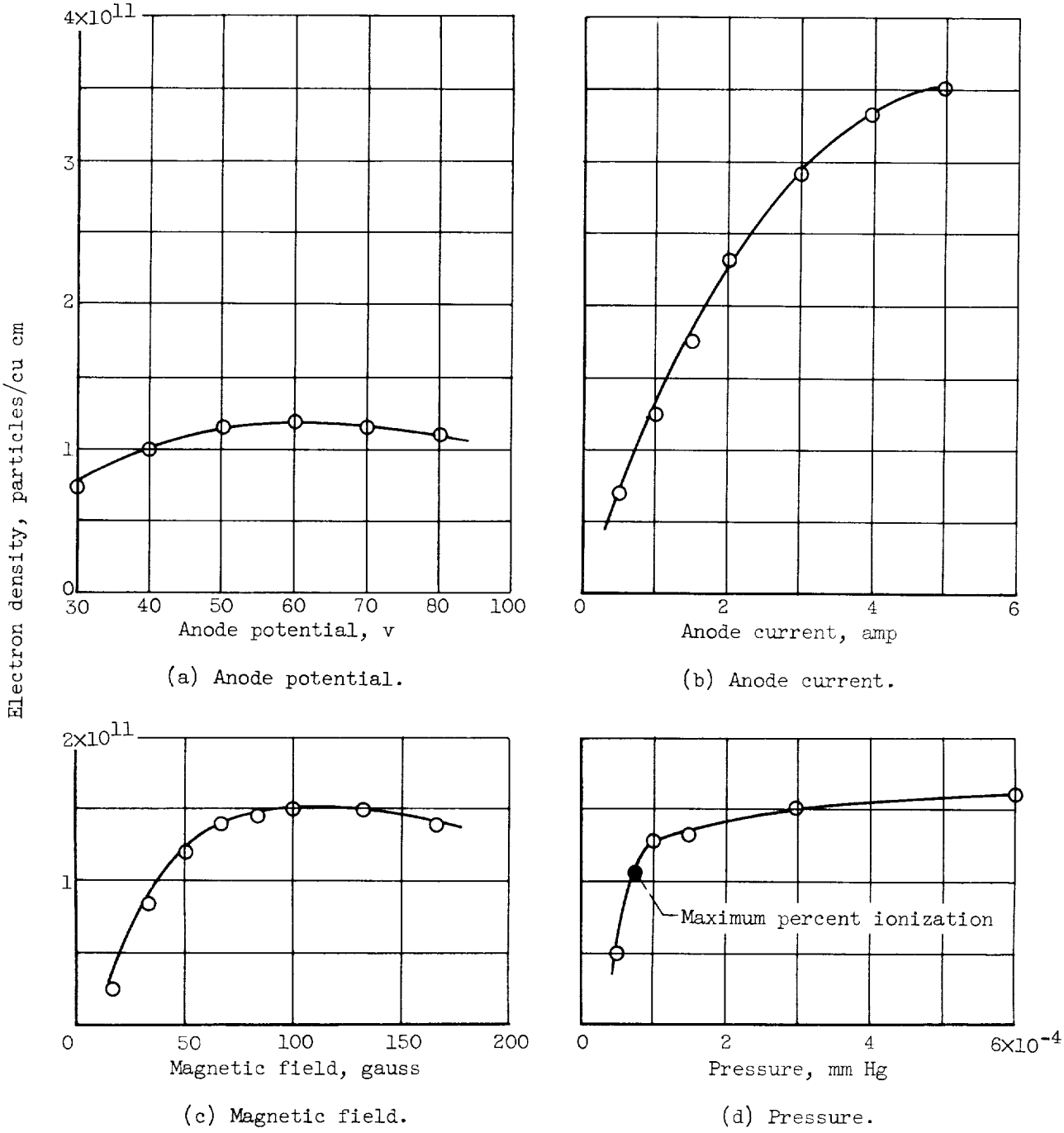

Figure 7. - Typical variation of number density as function of discharge parameters; center of pipe 1 inch from source. Values of discharge parameters except when displayed as the variable: anode voltage, 50 volts; anode current, 1 ampere; magnetic field, 50 gauss; pressure, 1.5×10^{-4} millimeter mercury.

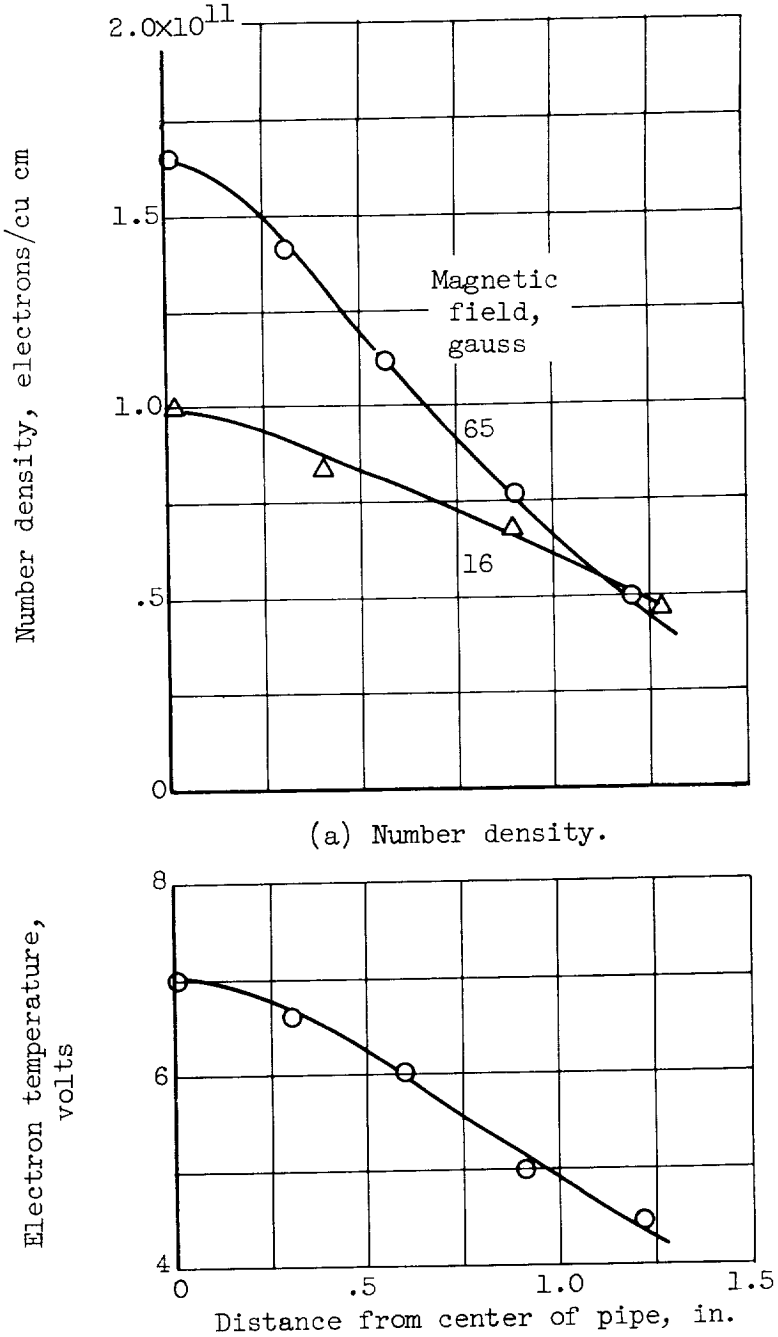

(a) Number density.

(b) Electron temperature.

Figure 8. - Radial variation of number density and temperature 1 inch from source. Anode potential, 50 volts; anode current, 1 ampere; magnetic field, 50 gauss; pressure, 1.5×10^{-4} millimeter mercury.

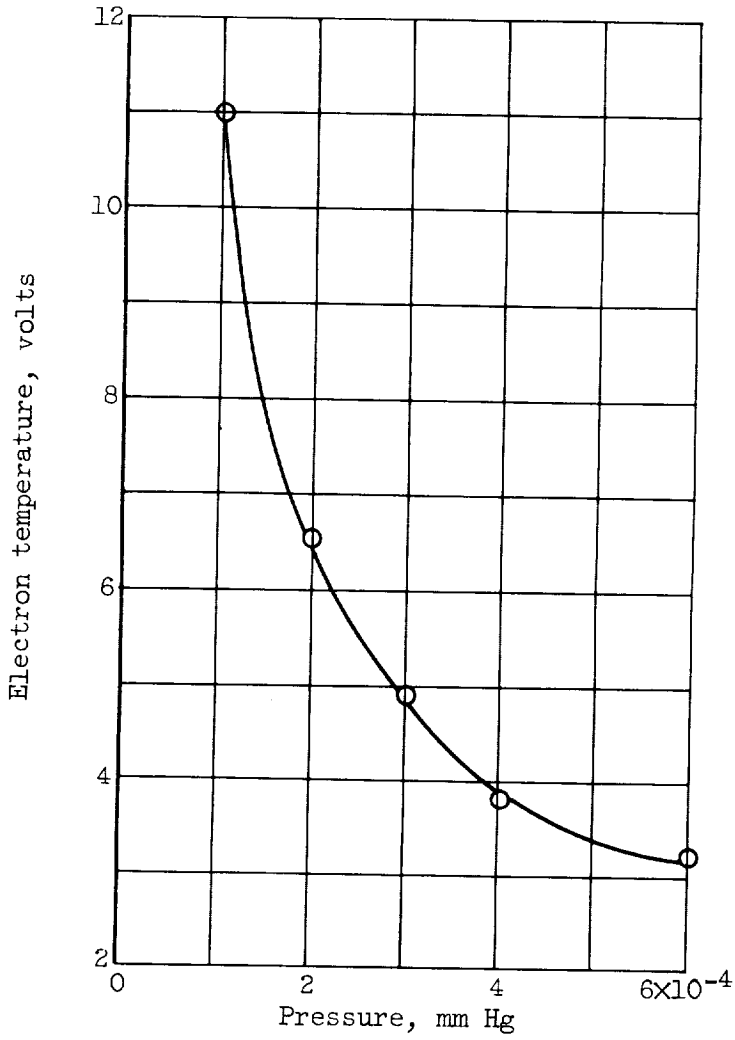

Figure 9. - Electron temperature as function of pressure. Center of pipe 1 inch from source; anode potential, 50 volts; anode current, 1 ampere; magnetic field, 50 gauss.

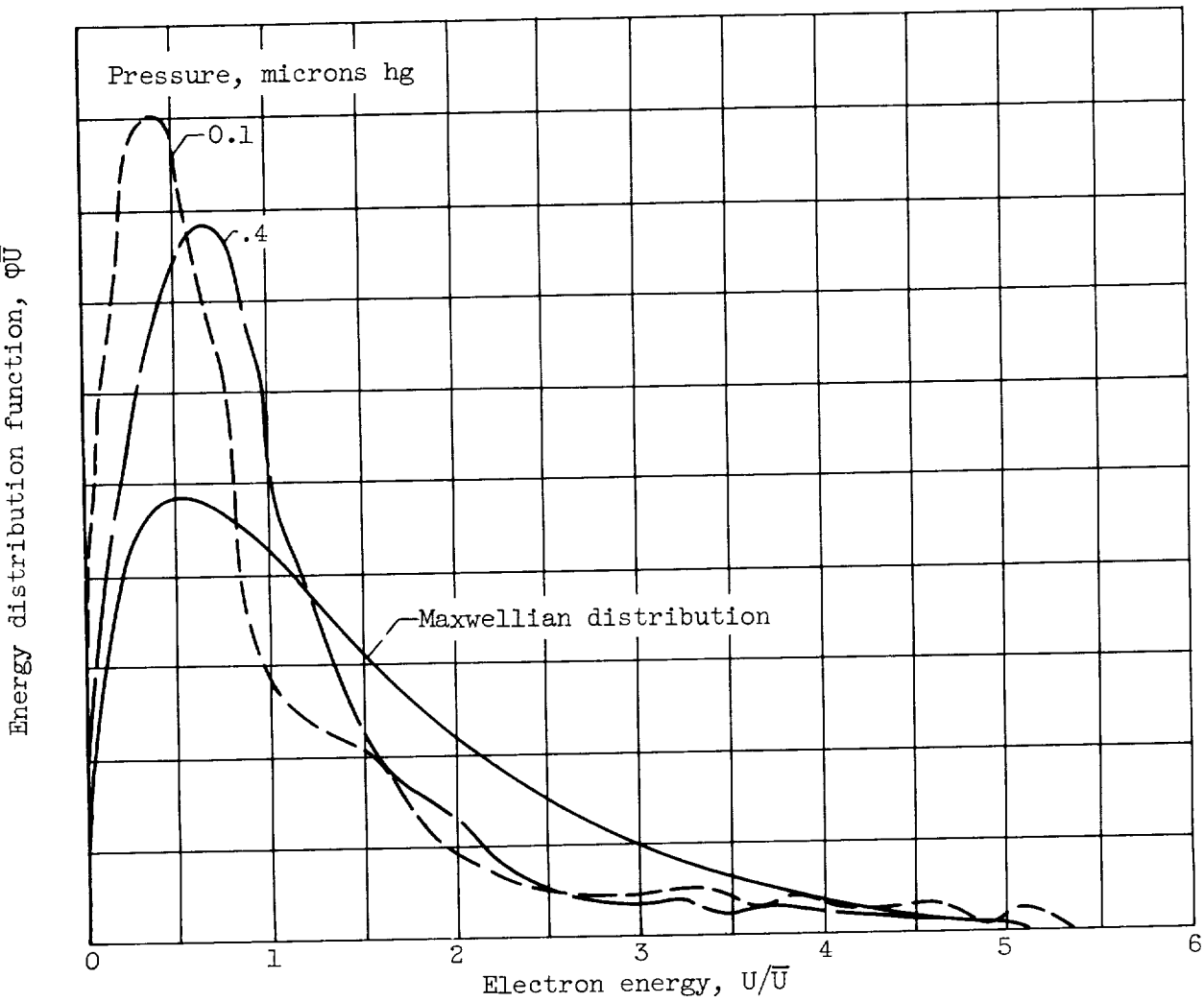

Figure 10. - Electron energy distribution (normalized). Center of pipe 1 inch from source; anode potential, 50 volts; anode current, 0.5 ampere; magnetic field, 25 gauss. $\int_0^\infty \varphi\bar{U}\, d\left(\frac{U}{\bar{U}}\right) = 1.$

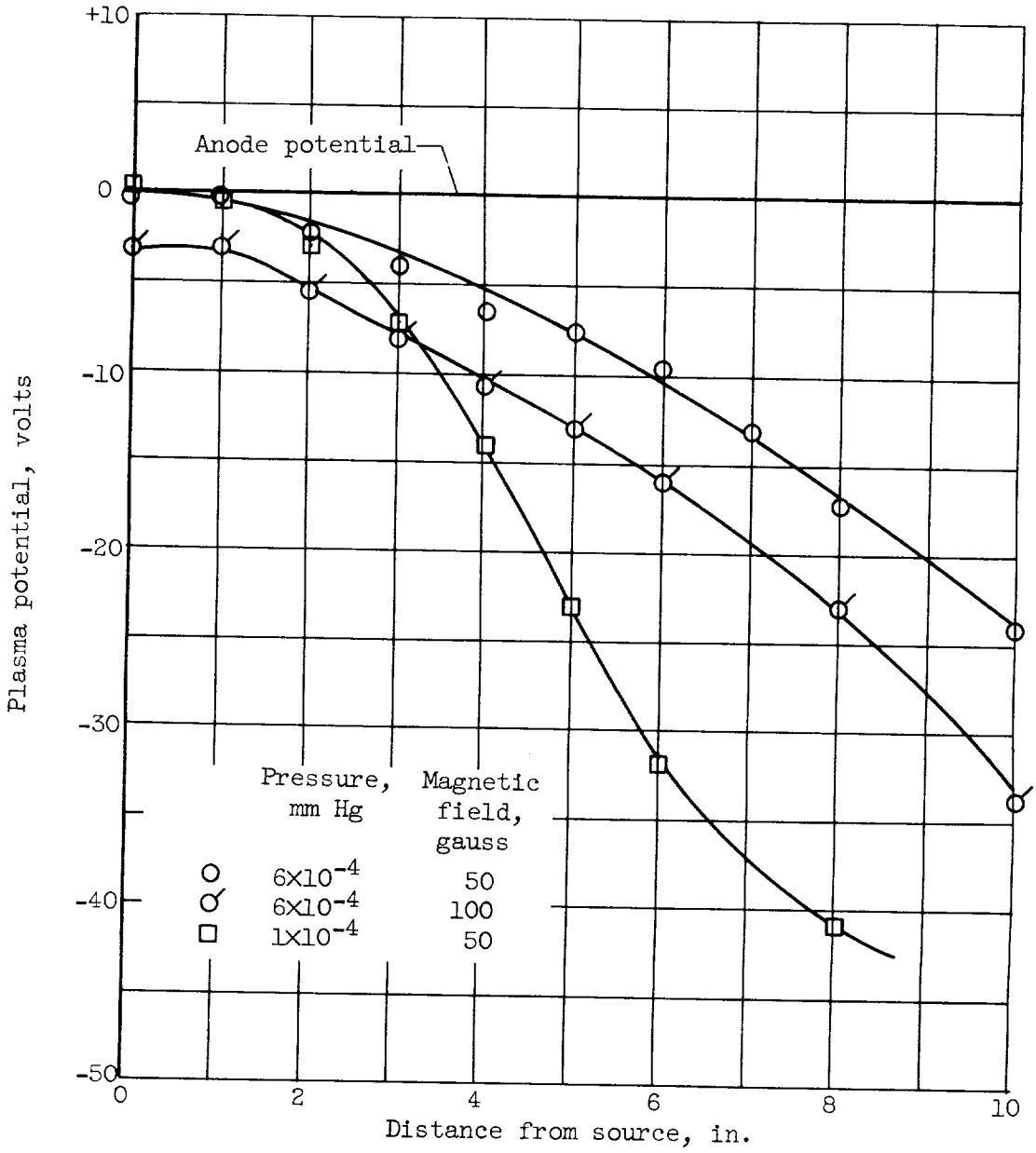

Figure 11. - Axial plasma potential along centerline of pipe.

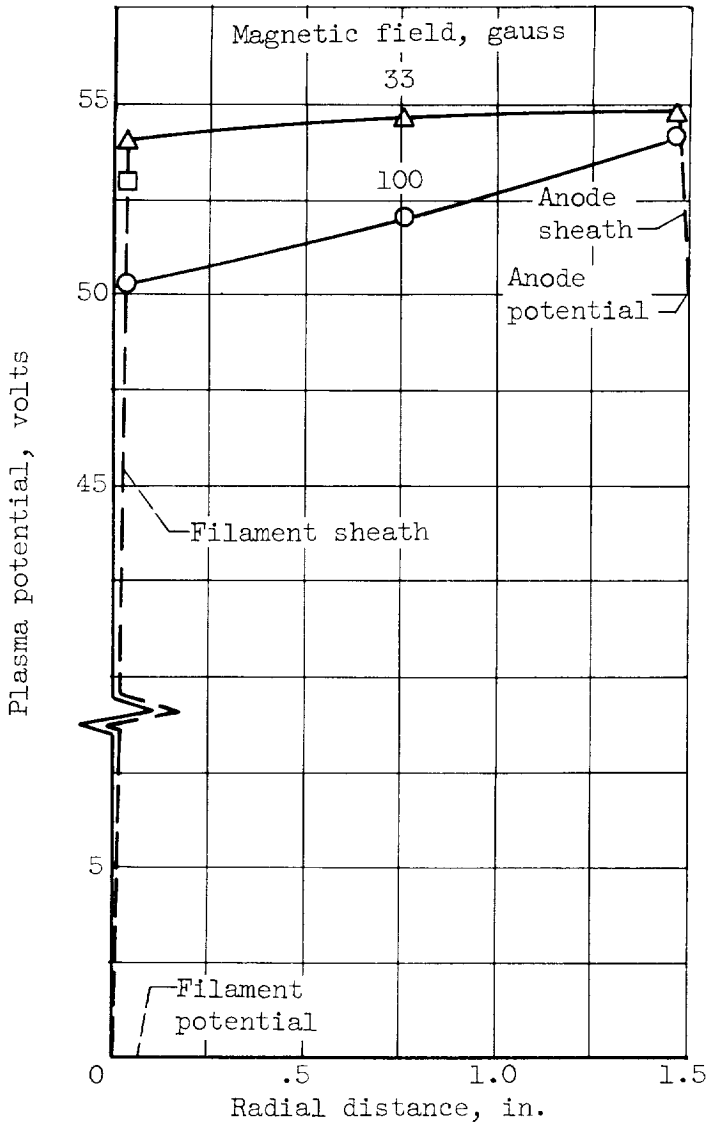

Figure 12. - Radial potential inside plasma source. Anode current, 1 ampere; pressure, 1.5×10^{-4} millimeter mercury.

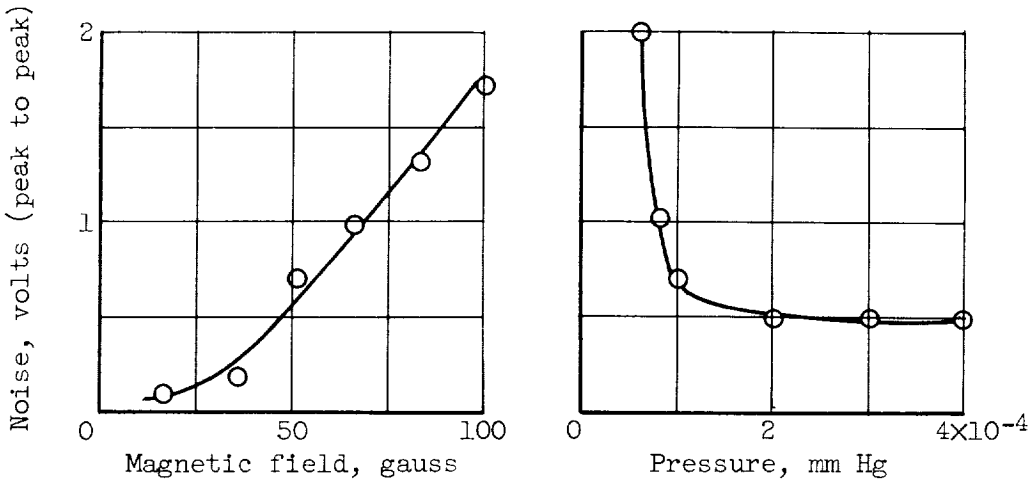

(a) Pressure, 1×10^{-4} millimeter mercury.

(b) Anode potential, 60 volts; anode current, 1 ampere; magnetic field, 50 gauss.

Figure 13. - Noise as a function of magnetic field and pressure 1 inch from source.

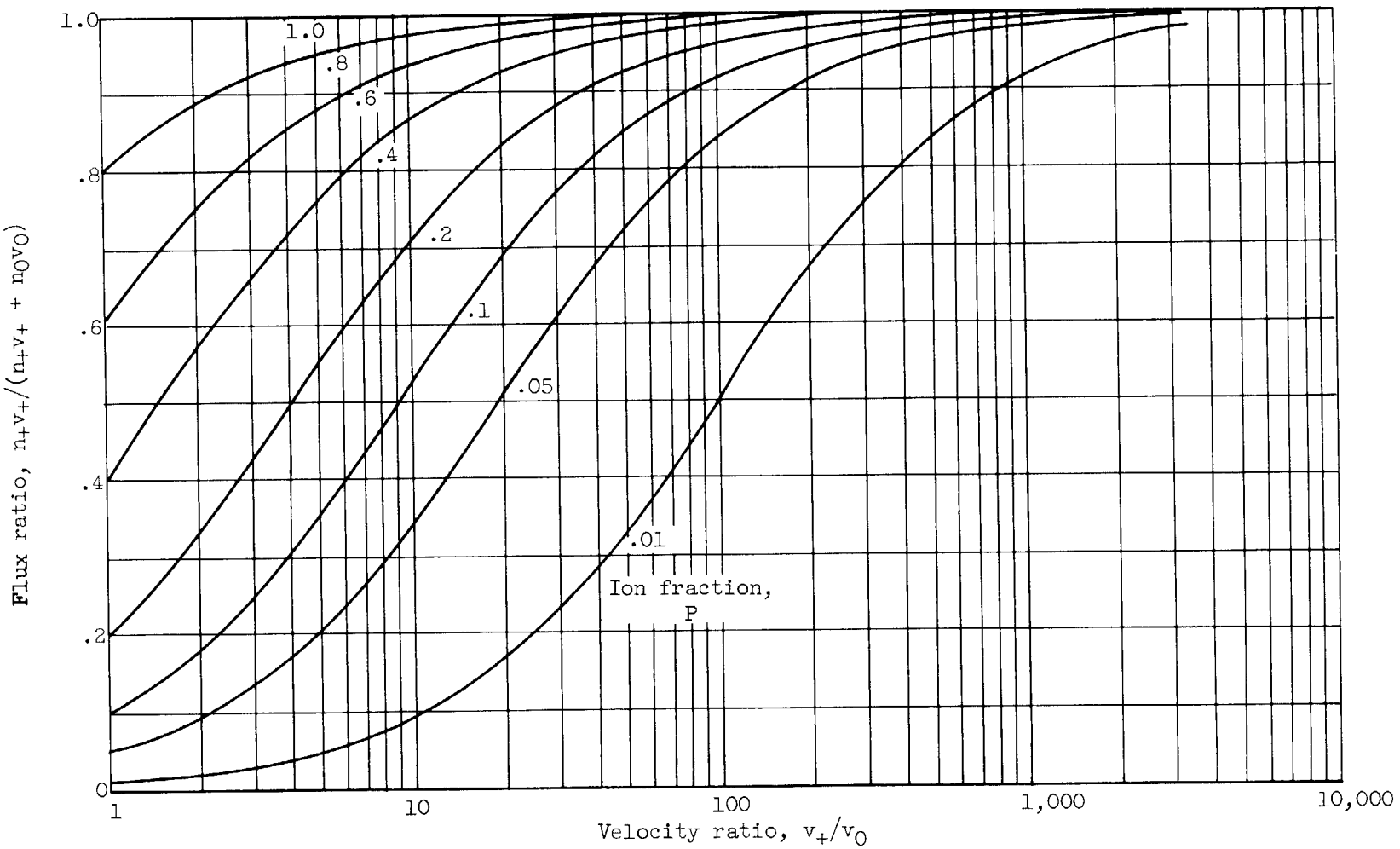

Figure 14. - Flux ratio as function of ion to neutral velocity ratio with ionized fraction P as a parameter.

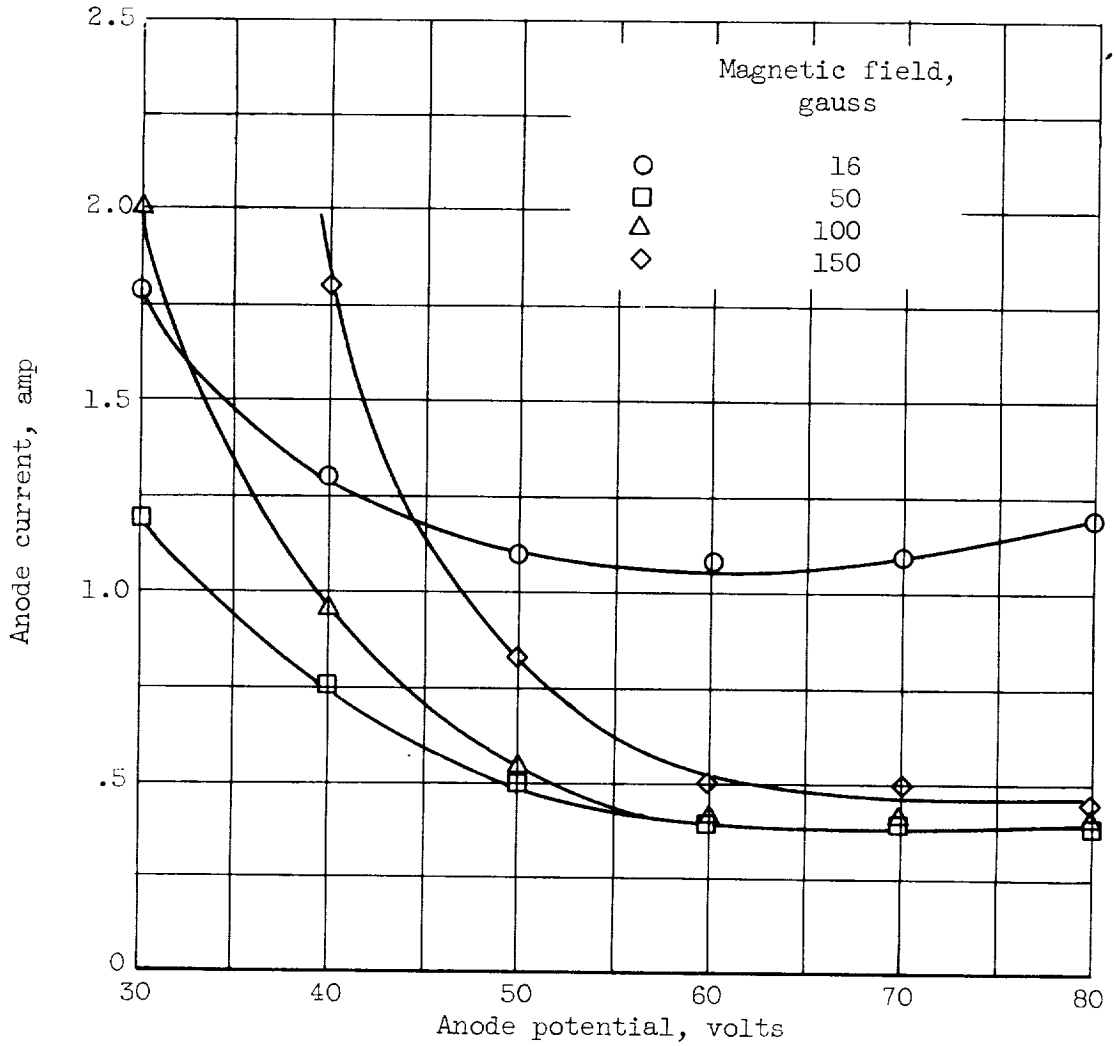

Figure 15. - Variation of discharge parameters at constant pressure and constant collected current. Total plasma probe current, 0.200 ampere; pressure, 3×10^{-4} millimeter mercury.

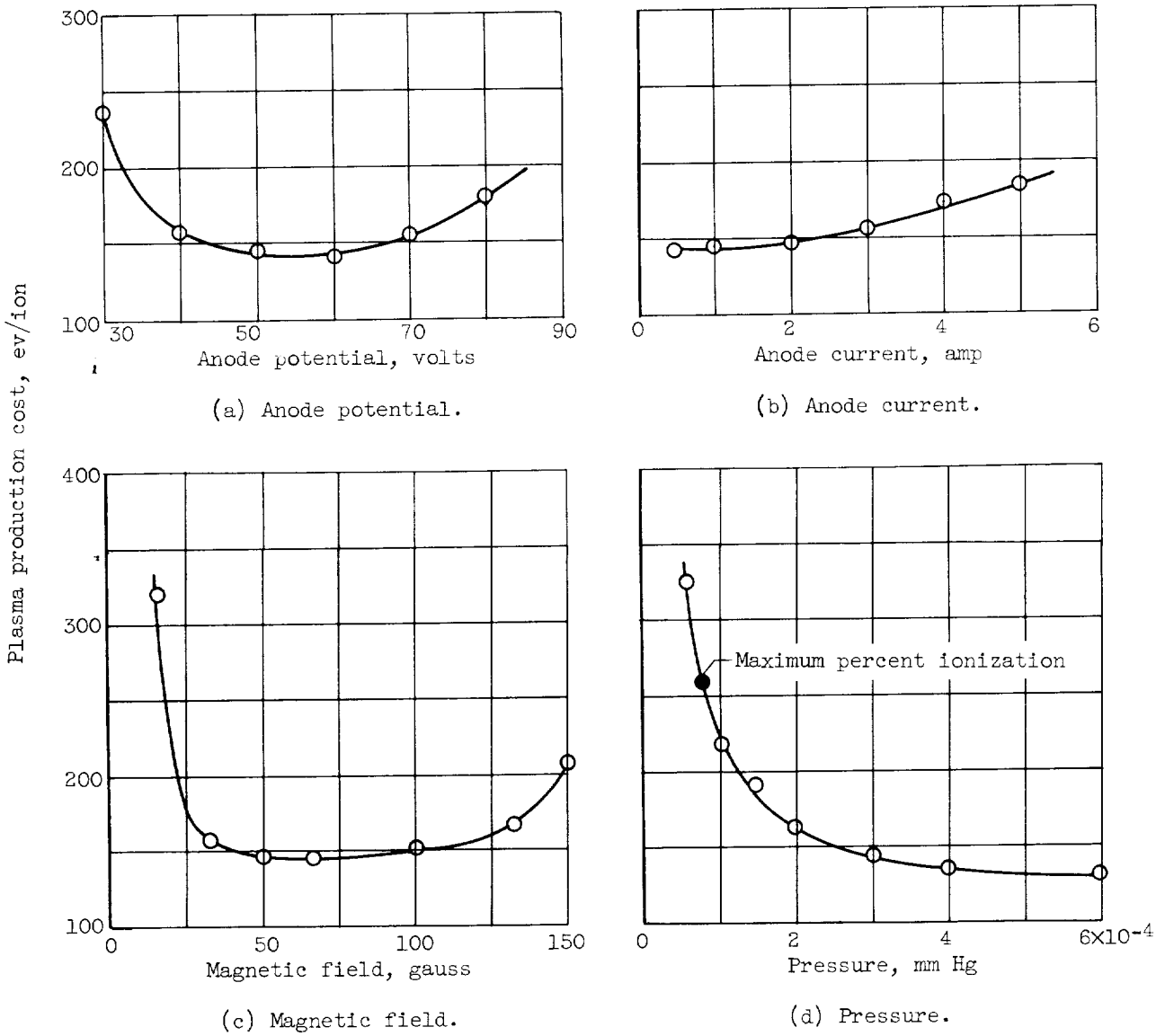

Figure 16. - Plasma production cost as function of discharge parameters. Values of discharge parameters except when displayed as the variable: anode potential, 50 volts; anode current, 1 ampere; magnetic field, 50 gauss; pressure, 3×10^{-4} millimeter mercury.